Three flavor Nambu-Jona Lasinio model with Polyakov loop and competition with nuclear matter

M. Ciminale,[1, 2, *] R.Gatto,[3, †] N. D. Ippolito,[1, 2, ‡] G. Nardulli,[1, 2, §] and M. Ruggieri[1, 2, ¶]

[1]Università di Bari, I-70126 Bari, Italia
[2]I.N.F.N., Sezione di Bari, I-70126 Bari, Italia
[3]Département de Physique Théorique, Université de Genève, CH-1211 Genève 4, Suisse

We study the phase diagram of the three flavor Polyakov-Nambu-Jona Lasinio (PNJL) model and in particular the interplay between chiral symmetry restoration and deconfinement crossover. We compute chiral condensates, quark densities and the Polyakov loop at several values of temperature and chemical potential. Moreover we investigate on the role of the Polyakov loop dynamics in the transition from nuclear matter to quark matter.

I. INTRODUCTION

A long-standing problem with Quantum Chromodynamics (QCD) is the difficulty of an analytical study in the nonperturbative regime. To deal with this issue a few approximate approaches have been developed, based on the idea of effective field theories. Among them, the Nambu-Jona Lasinio model [1] (NJL in the following) has become a popular tool to describe some of the salient aspects of low energy QCD, in particular chiral symmetry breaking and its restoration at high density and/or temperature (see Refs. [2] for reviews).

The NJL model neglects the gluon dynamics, the interactions among quarks being described by contact terms. Due to the absence of gluons, one of the main properties of low-energy QCD at small temperature and baryonic density, namely confinement, is missing in this effective description. This defect not-withstanding, the NJL model enjoys a significant popularity since it allows analytical treatments in different contexts. In order to cure its deficiencies some extensions have been also proposed. They either try to describe quarks and hadrons in unified approaches (see Ref. [3] and references therein), or add a bag constant to the equation of state of the NJL quark matter [4]. In the latter procedure the deconfinement transition is obtained by computing the pressure of nuclear matter at low density and temperature by some effective model and comparing it to the pressures of the quark matter. When the nuclear matter pressure becomes smaller than the quark pressure, deconfinement is energetically favored. We stress that the introduction of a bag constant is needed to reproduce the phase transition from the nuclear to the quark phase in this approach.

Another extension of the NJL model has been suggested in Ref. [5]. In this paper part of the gluon dynamics is described by a background temporal gluon field coupled to quarks by the QCD covariant derivative. The background field adds a potential term $\mathcal{U}(\Phi)$ to the lagrangian. Its value is determined for any temperature T and quark chemical potential μ by the minimization of the effective potential and depends on the traced Polyakov loop Φ [6], related to the background gauge field. The resulting model is known as Polyakov-Nambu-Jona Lasinio (PNJL) model.

As is well known the Polyakov loop in a pure gauge theory is an order parameter of the deconfinement transition [6]. This peculiarity is related to the existence of a discrete symmetry Z_3 of the pure gauge action, which is spontaneously broken when deconfinement sets in. The Polyakov loop vanishes in the disordered low temperature phase and is different from zero in the high T phase. When dynamical quarks are added, Z_3 symmetry is explicitly broken and Φ can no longer be considered as an order parameter. However, as shown by lattice simulations, its behavior as a function of T (increasing from zero to non vanishing values when T increases) can still describe the deconfinement crossover. One might assume that this happens also when the chemical potential μ is varied, which should show a link between deconfinement and chiral restoration [7, 8]. Therefore in the PNJL model, one introduces a Polyakov loop dynamics in the NJL model trying to reproduce both chiral symmetry breaking and quark confinement.

The PNJL model with two flavors has been extensively studied [9, 10, 11, 12, 13, 14, 15, 16]. In Ref. [17] an extension to the three flavor model has been considered, by studying the effects of the Polyakov loop on the thermodynamics

of the Color-Flavor-Locked phase of high density QCD [18] near its second order transition to the normal phase. The aim of this paper is to extend this analysis to moderate densities. In particular we will study the phase diagram of the three flavor PNJL model and the transition from nuclear to deconfined quark matter. We shall consider massive quarks because, differently from previous work [17], mass effects cannot be neglected at moderate values of the quark chemical potential. Therefore we introduce bare quark masses and also compute selfconsistently their in-medium values in the mean field approximation. On the other hand, since we are mainly interested in the interplay of chiral symmetry restoration and deconfinement crossover we neglect the possibility of color superconductivity, which should be produced at higher densities [19, 20, 21, 22]. While chiral symmetry restoration is adequately described by the PNJL model, to establish the deconfinement transition we have to consider also nuclear matter, described by an effective field theory, so that a comparison of free energies can be made.

The plan of the paper is as follows. In Section II we summarize the main features of the three flavor PNJL model. Section III is devoted to the study of the phase diagram of the model. In Section IV we compare PNJL quark matter with nuclear matter. Finally, in Section V we draw our conclusions.

II. THERMODYNAMICS OF THE THREE FLAVOR PNJL MODEL

We consider the lagrangian

$$\mathcal{L} = \sum_f \bar{\psi}_f \left(iD_\mu \gamma^\mu - m_f + \mu \gamma_0 \right) \psi_f + \mathcal{L}_4 + \mathcal{L}_6 , \tag{1}$$

where the sum is over the three flavors f ($= 1, 2, 3$ for u, d, s). In the above equation we have introduced the coupling of the quarks to a background gauge field $A_\mu = g\delta_{\mu 0}A_{a\mu}T_a$ via the covariant derivative $D_\mu = \partial_\mu - iA_\mu$; m_f is the current mass (we assume $m_u = m_d$). The quark chemical potential is denoted by μ. The NJL four-fermion and six-fermion interaction Lagrangians are as follows [2]:

$$\mathcal{L}_4 = G \sum_{a=0}^{8} \left[\left(\bar{\psi}\lambda_a\psi \right)^2 + \left(i\bar{\psi}\gamma_5\lambda_a\psi \right)^2 \right] , \tag{2}$$

$$\mathcal{L}_6 = -K \left[\det\bar{\psi}_f(1+\gamma_5)\psi_{f'} + \det\bar{\psi}_f(1-\gamma_5)\psi_{f'} \right] , \tag{3}$$

where λ_a are the Gell-Mann matrices in flavor space ($\lambda_0 = \sqrt{2/3}\,\mathbf{1}_f$) and the determinant is in flavor space as well. Working in the mean field approximation the self-consistent equations for the constituent quark masses are

$$M_f = m_f - 4G\sigma_f + 2\,K\,\sigma_{f+1}\,\sigma_{f+2} ; \tag{4}$$

here $\sigma_f = \langle \bar{f}f \rangle$ denotes the chiral condensate of the flavor f, and we define $\sigma_4 = \sigma_u$, $\sigma_5 = \sigma_d$. We also introduce the quark mass matrix $M = \text{diag}[M_u, M_d, M_s]$. The gap equation at $T = 0$ and $\mu = 0$ is

$$\sigma_f = -\frac{3M_f}{\pi^2} \int_0^\Lambda \frac{p^2}{\sqrt{p^2 + M_f^2}} \, dp , \tag{5}$$

which depends on the ultraviolet cutoff Λ. The parameters are chosen as in Ref. [20], i.e.

$$m_{u,d} = 5.5 \text{ MeV} , \ m_s = 140.7 \text{ MeV} , \ G\Lambda^2 = 1.835 , \ K\Lambda^5 = 12.36 , \ \Lambda = 602.3 \text{ MeV} . \tag{6}$$

By these parameters one gets $m_\pi \simeq 135$ MeV, $m_K \simeq 498$ MeV, $m_{\eta'} \simeq 958$ MeV, $m_\eta \simeq 515$ MeV and $f_\pi \simeq 92$ MeV.

Once the lagrangian is specified, the thermodynamic potential at temperature T is obtained after integration over the fermion fields in the partition function:

$$\Omega = \mathcal{U}[T, \Phi, \bar{\Phi}] + 2G \sum_{f=u,d,s} \sigma_f^2 - 4K\sigma_u\sigma_d\sigma_s - T \sum_n \int \frac{d^3p}{(2\pi)^3} \text{Tr} \log \frac{S^{-1}(i\omega_n, \boldsymbol{p})}{T} . \tag{7}$$

Here $\omega_n = \pi T(2n+1)$ are Matsubara frequencies. The inverse quark propagator is given in momentum space by

$$S^{-1} = \gamma_0 \left(p^0 + \mu - iA_4 \right) - \boldsymbol{\gamma} \cdot \boldsymbol{p} - M , \tag{8}$$

where $A_4 = iA_0$. A most significant difference between the NJL and the PNJL model is the presence in the thermodynamic potential of the gluon contribution $\mathcal{U}(T, \Phi, \bar{\Phi})$ describing the dynamics of the traced Polyakov loop

$$\Phi = \frac{1}{3}\mathrm{Tr}_c \mathcal{P} \exp\left[i \int_0^\beta d\tau A_4(\boldsymbol{x}, \tau)\right] \ , \qquad \bar{\Phi} = \frac{1}{3}\mathrm{Tr}_c \mathcal{P} \exp\left[-i \int_0^\beta d\tau A_4^\star(\boldsymbol{x}, \tau)\right] \ , \tag{9}$$

in absence of dynamical quarks. We will consider in the following two different choices of the potential. First we assume a polynomial expansion in Φ and $\bar{\Phi}$:

$$\text{Polynomial model}: \qquad \frac{\mathcal{U}[T, \Phi, \bar{\Phi}]}{T^4} = -\frac{b_2(T)}{2}\bar{\Phi}\Phi - \frac{b_3}{6}\left(\Phi^3 + \bar{\Phi}^3\right) + \frac{b_4}{4}(\bar{\Phi}\Phi)^2 \ , \tag{10}$$

where

$$b_2(T) = a_0 + a_1\left(\frac{T_0}{T}\right) + a_2\left(\frac{T_0}{T}\right)^2 + a_3\left(\frac{T_0}{T}\right)^3 \ . \tag{11}$$

This corresponds to the choice $\theta = 0$ for the parameter θ introduced in [13]. Numerical values of the coefficients are [9]

$$a_0 = 6.75, \quad a_1 = -1.95, \quad a_2 = 2.625, \quad a_3 = -7.44 \ , \quad b_3 = 0.75 \ , \quad b_4 = 7.5 \ . \tag{12}$$

The remaining parameter T_0 is the deconfinement temperature of static and infinitely heavy quarks [6]. This parameter depends in principle on the number of flavors and on the quark chemical potential. We shall investigate two cases. First, we assume a constant value $T_0 = 270$ MeV, which corresponds to the deconfinement temperature of static and infinitely heavy quarks as computed in lattice QCD (see for example [10]). The second case we study is the μ-dependent T_0 suggested in [13],

$$T_0 = T_\tau e^{-1/(\alpha_0 b(\mu))} \ , \tag{13}$$

with $T_\tau = 1770$ MeV, $\alpha_0 = 0.304$ and

$$b(\mu) = \frac{1}{6\pi}(11N_c - 2N_f) - \frac{16}{\pi}N_f\frac{\mu^2}{T_\tau^2} \tag{14}$$

(this dependence is motivated by the use of hard dense loop and hard thermal loop results for the effective charge [13, 23]). The prescription in (13) gives $T_0 = 178$ MeV at $\mu = 0$.

The second model we consider uses instead of (10) the following logarithmic form

$$\text{Logarithmic model}: \qquad \frac{\mathcal{U}(T, \Phi, \bar{\Phi})}{T^4} = -\frac{\tilde{b}_2(T)}{2}\bar{\Phi}\Phi + b(T)\ln[1 - 6\bar{\Phi}\Phi + 4(\Phi^3 + \bar{\Phi}^3) - (\bar{\Phi}\Phi)^2] \tag{15}$$

with

$$\tilde{b}_2(T) = \tilde{a}_0 + \tilde{a}_1\left(\frac{T_0}{T}\right) + \tilde{a}_2\left(\frac{T_0}{T}\right)^2 \ , \quad b(T) = \tilde{b}_3\left(\frac{T_0}{T}\right)^3 \ . \tag{16}$$

Numerical values of the coefficients are as follows [10]

$$\tilde{a}_0 = 3.51, \quad \tilde{a}_1 = -2.47, \quad \tilde{a}_2 = 15.2, \quad \tilde{b}_3 = -1.75 \ . \tag{17}$$

In this second case we only consider the case of a fixed value of T_0: T_0=183 MeV, corresponding to the $N_f = 3$ value of the deconfinement temperature estimated in Ref. [13].

Evaluation of the trace gives in both cases for the thermodynamic potential the expression

$$\begin{aligned}
\Omega \ = \ &\mathcal{U}[T, \Phi, \bar{\Phi}] + 2G \sum_{f=u,d,s} \sigma_f^2 - 4K\sigma_u\sigma_d\sigma_s - 6 \sum_{f=u,d,s} \int \frac{d^3p}{(2\pi)^3} E_f \ \theta(\Lambda - |\boldsymbol{p}|) \\
&-2T \sum_{f=u,d,s} \int \frac{d^3p}{(2\pi)^3} \log\left[1 + 3\Phi e^{-\beta(E_f-\mu)} + 3\bar{\Phi}e^{-2\beta(E_f-\mu)} + e^{-3\beta(E_f-\mu)}\right] \\
&-2T \sum_{f=u,d,s} \int \frac{d^3p}{(2\pi)^3} \log\left[1 + 3\bar{\Phi}e^{-\beta(E_f+\mu)} + 3\Phi e^{-2\beta(E_f+\mu)} + e^{-3\beta(E_f+\mu)}\right] \ ,
\end{aligned} \tag{18}$$

with $E_f = \sqrt{\boldsymbol{p}^2 + M_f^2}$ and M_f given by Eq. (4). By searching the global minimum of Ω one can get quark condensates σ_f and Polyakov loop for any values of the parameters μ and T.

III. NUMERICAL RESULTS

In Fig. 1 we show the phase diagrams of three cases mentioned above (two cases for the polynomial model, one for the logarithmic model). They are obtained as follows. For any value of the quark chemical potential, the critical temperature is identified with the temperature at which the up quark chiral condensate σ_u has a jump (first order transition), or the derivative of σ_u with respect to the temperature is maximum (second order transition). The phase
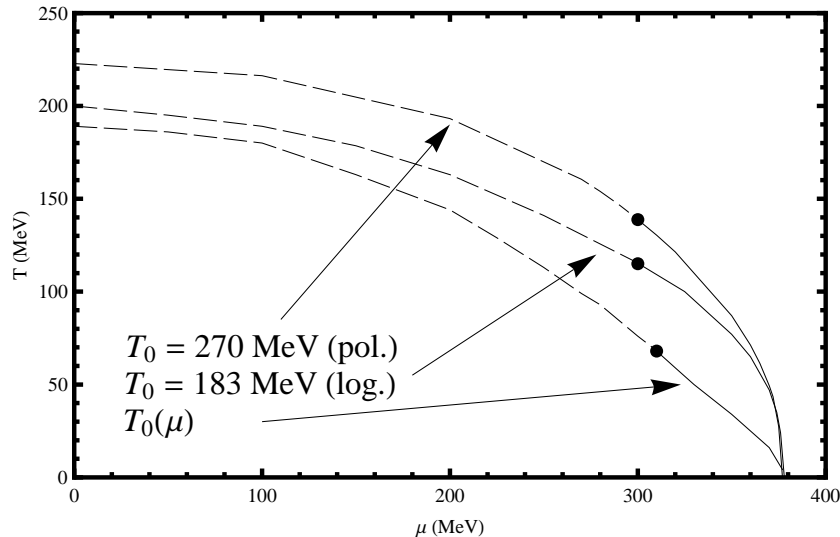

FIG. 1: Phase diagram of the PNJL model. The three lines correspond to the following models: T_0 fixed at the constant value 270 MeV and polynomial form for the Polyakov potential $\mathcal{U}(\Phi)$ (highest); $T_0 = 183$ MeV and logarithmic form of the potential (middle); $T_0 = T_0(\mu)$ and polynomial form (lowest). A solid line denotes a first order chiral transition, a dashed line a cross-over for the condensate $< \bar{u}u >$ and a bold point a critical endpoint (CEP).

diagrams of the polynomial model correspond to the highest and lowest lines, while the intermediate line is obtained by the logarithmic potential. The two lines of the polynomial model are obtained with the fixed value $T_0 = 270$ MeV (upper line) and with $T_0(\mu)$ of Eq. (13) (lower) respectively. Qualitatively the three curves are similar, which shows the physical results are insensitive to the details of the model. The critical endpoints (CEPs) separating the cross-over from the first-order lines are located, for the three cases, at $(\mu_E, T_E) \approx (300, 140)$ MeV (highest curve), $(\mu_E, T_E) \approx (300, 115)$ MeV (middle curve) $(\mu_E, T_E) \approx (310, 68)$ MeV (lowest curve). At $\mu = 0$ we find for the three cases the cross-over temperatures $T_\chi(\mu = 0) \approx 223$ MeV (highest curve), $T_\chi(\mu = 0) \approx 200$ MeV (middle curve), $T_\chi(\mu = 0) \approx 189$ MeV (lowest curve).

The numerical values of the cross-over temperatures at $\mu = 0$ are in the same range of the results found in QCD-like theories [24, 25, 26] or in lattice QCD [27]. On the other hand, the CEPs are located at values of μ much higher than the respective values found in QCD/like theories [24, 25, 26], lattice QCD [27] and empirical analysis of the ratio of shear viscosity to entropy density [28], which suggest there is a CEP at $T \approx 165$ MeV and $\mu \approx 50$ MeV. Clearly the details of the models matter; in relation to this problem, in Ref. [12] an extension of the PNJL model (in the case of two flavors) has been proposed using also a $\mathcal{O}(\bar{\psi}\psi)^4$ interaction term. It was found that the effect of the new kind of interaction is to locate the critical end point at higher temperature and lower chemical potential than the NJL/PNJL results. One might expect similar effects in the three flavor models considered in the present paper.

The phase diagrams in Fig. 1 are based on the results of Fig. 2 that shows the $T-$ dependence (at fixed μ) of the chiral condensates. The u chiral condensates are represented by dashed lines, those of the strange quark by dot-dashed lines (solid lines represent the Polyakov loop Φ). We have reported results only for the polynomial model for the two cases of fixed $T_0 = 270$ MeV (upper panels) and $T_0(\mu)$ (lower panels), since the results for the case of the logarithmic potential are qualitatively similar to those of the case of the polynomial potential with $T_0 = 270$ MeV. On the right panel of Fig. 2 we have results at $\mu = 350$ MeV, on the left those at $\mu = 150$ MeV.

From the diagrams of Fig. 2 we can identify another relevant transition temperature: T_Φ, i.e. the temperature corresponding to the inflection point of Φ (defined as the temperature where $d\Phi/dt$ has a maximum). As discussed in the introduction T_Φ cannot be immediately interpreted as the deconfinement temperature because Z_3 is not a symmetry of QCD with dynamical quarks. In fact in the next section we shall adopt a different method to study the deconfinement transition, based on the comparison of the pressures of the two competing states of matter (quark
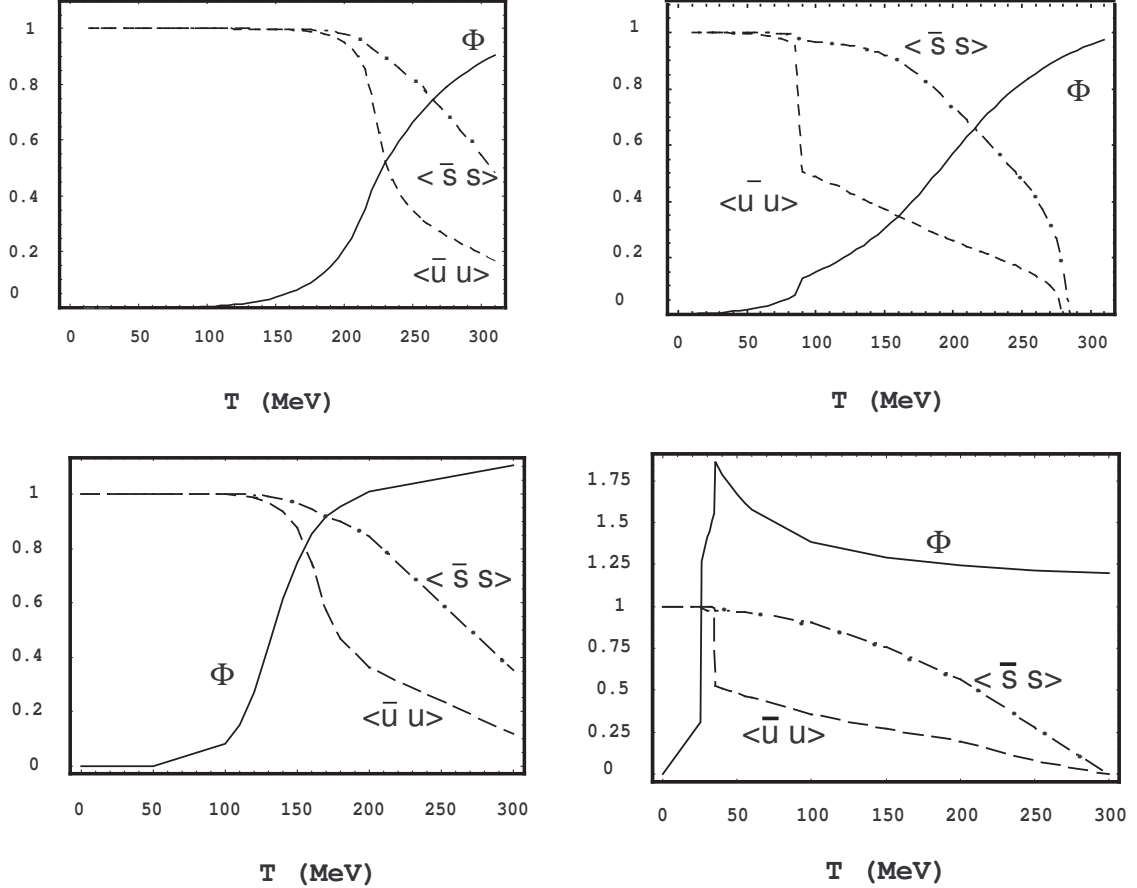
FIG. 2: Upper panels: Polyakov loop Φ (solid line) and chiral condensates for u quark (dashed line) and s quark (dot-dashed line) versus temperature in MeV, at $\mu = 150$ MeV (left) and $\mu = 350$ MeV (right), for the PNJL model with fixed $T_0 = 270$ MeV. For each value of μ the condensates are normalized to their values at $T = 0$. Lower panels: Same quantities for the model with $T_0 = T_0(\mu)$.

and nuclear). Nevertheless T_Φ should approximately coincide with the deconfinement transition, if the guess on the relevance of the rise of Polyakov loop for the deconfinement of dynamical quarks is correct. One can note a different behavior between the two cases $T_0 = 270$ MeV (fixed) and $T_0(\mu)$. In the former case T_Φ numerically coincides either with the chiral crossover (at low μ) or with the chiral first order phase transition (high μ). In the latter case this equality is lost, the shift between T_ϕ and T_χ being of the order of 30 MeV for μ in the interval $[0, 320]$ MeV, and shrinking as μ is increased above 320 MeV. Another peculiarity of the $T_0(\mu)$ case is that at high temperatures $\Phi > 1$. This is not acceptable since Φ is defined as the normalized trace of a $SU(3)$ matrix and should therefore lie in the interval $0 \leq |\Phi| \leq 1$. The fact that $|\Phi|$ can be larger than one in the PNJL model with a polynomial potential is well known in the two flavor case [9], and to solve this problem several improvements have been suggested, e.g the use of the logarithmic potential [5, 10] or the interpretation of the Polyakov loop potential as a random matrix model [11, 29, 30]. In our numerical calculations within the logarithmic potential model we have checked that $|\Phi|$ is always less than one.

Another possible signature of the deconfinement transition is offered by the behavior of the quark number densities. In Fig. 3 we show the results for the scaled quark number densities $\tilde{n}_f$. For each flavor f, $\tilde{n}_f$ is defined as follows:

$$\tilde{n}_f \equiv \frac{n_f}{T^3} = -\frac{1}{T^3}\frac{\partial\Omega}{\partial\mu_f} \ . \tag{19}$$

We plot $\tilde{n}_f$ as a function of T at $\mu = 150$ MeV (left) and $\mu = 350$ MeV (right) for the two cases $T_0 = 270$ MeV and $T_0(\mu)$. At fixed quark chemical potential the quark number density is almost vanishing below the chiral transition temperature, rising quickly in proximity of the transition itself. This behavior has been interpreted in the two flavor
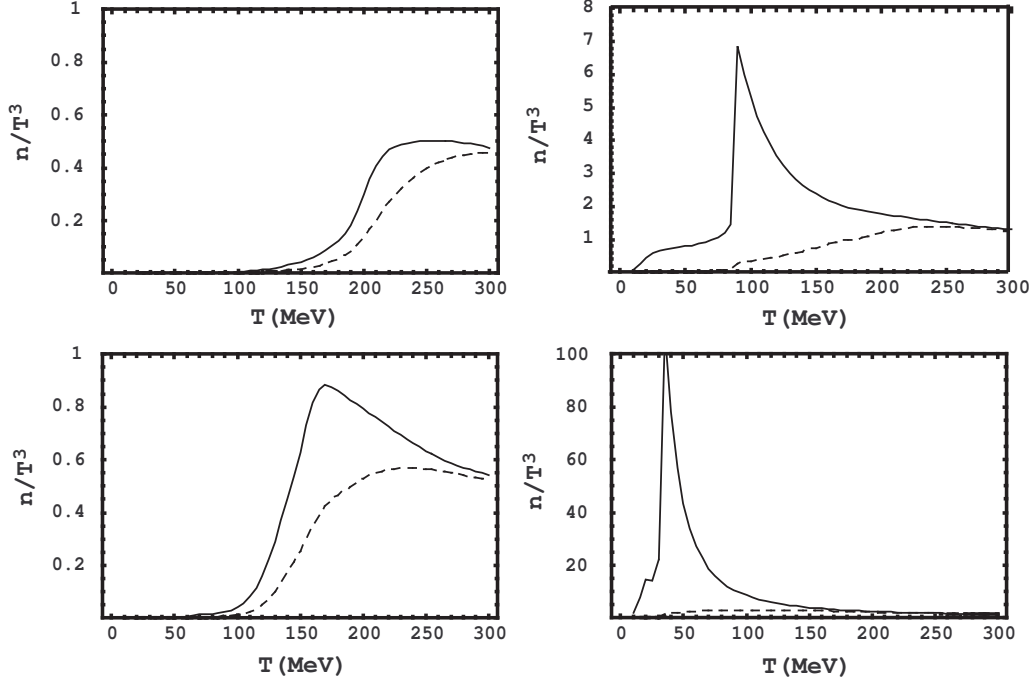
FIG. 3: Upper panels: scaled number densities of quarks n/T^3 versus temperature (MeV) at $\mu = 150$ MeV (left) and $\mu = 350$ MeV (right) calculated in the PNJL model with fixed $T_0 = 270$ MeV; solid lines correspond to up and down quarks, dashed lines to the strange quark. Lower panels: the same quantities for the model with $T_0 = T_0(\mu)$.

case as a simulation of the confined→deconfined transition in the PNJL model [9].

IV. COMPARISON WITH NUCLEAR MATTER

We shall try here to confront the previous calculations with a concrete phenomenological model for the transition from nuclear matter to quark matter. The model will be based on a rather rough modelisation, but we shall see that the emerging pattern will still not be very far from that suggested in our previous analysis. In order to locate more accurately the deconfinement transition, as well as to study its nature, we now examine the pressure of a gas made by hadrons at small temperature and small baryonic chemical potential $\mu_B = 3\mu$ and compare it to the pressure of the PNJL model, the transition occurring when the difference between the two pressures vanishes. Nuclear matter will be described by an effective model based on the non-linear extension of the original Walecka model [31] due to Boguta and Bodmer [32, 33] (WBB in the following). In its two-flavor version this model allows to predict both the compression modulus and the effective nucleon mass at saturation in agreement with their empirical values. The spinor content of the model we consider here is the whole lightest baryon octet. We will work assuming $SU(3)$ flavor symmetry for the couplings, but including mass differences in the baryon octet.

The effective Lagrangian of nuclear matter in the WBB model describes the baryons coupled to the σ scalar meson and the ω vector meson, and takes into account cubic and quartic self-interaction terms for the scalar field:

$$\mathcal{L} = \sum_B \bar{\psi}_B \left[i\gamma^\mu (\partial_\mu + i g_\omega \omega_\mu) - (M_B - g_\sigma \sigma) \right] \psi_B + \frac{1}{2} \left(\partial^\mu \sigma \partial_\mu \sigma - m_\sigma^2 \sigma^2 \right)$$
$$+ \ \frac{1}{2} m_\omega^2 \omega^\mu \omega_\mu - \frac{1}{4} \omega_{\mu\nu} \omega^{\mu\nu} - \frac{1}{3} b_M (g_\sigma \sigma)^3 + \frac{1}{4} c (g_\sigma \sigma)^4 \ . \tag{20}$$

In this equation $\omega_{\mu\nu} = \partial_\mu \omega_\nu - \partial_\nu \omega_\mu$ is the field strength tensor of ω. The fields for the σ and ω-mesons are denoted by σ, ω_μ respectively and ψ_B is the Dirac spinor for the baryon B having mass M_B (the sum over the index B is over the entire octet). Moreover g_σ, g_ω are the dimensionless coupling constants of the σ and ω fields; b_M and c are parameters; m_σ, m_ω are the masses of the σ, ω-mesons respectively. Values of the other parameters are in Table I.

	b_M/M_N	c	$(g_\sigma/m_\sigma)^2$ (fm^2)	$(g_\omega/m_\omega)^2$ (fm^2)
Set 1	1.46×10^{-2}	-1.24×10^{-2}	9.9262	4.233
Set 2	2.95×10^{-3}	-1.07×10^{-3}	11.79	7.15

TABLE I: Two sets of parameters for the nuclear matter effective lagrangian, see Eq. (20). We present results for the dimensionless constant b_M/M_N, related to the cubic interaction coupling constant b_M by the nucleon mass M_N.

We use two parameter sets. Set 1 corresponds to the softest nuclear equation of state discussed in [33]; Set 2 to the stiffest one. These parameters are identical to those used in the model with nucleons only (without hyperons). As discussed in [33] the use of the same parameters is justified since they are obtained by the fit of some nuclear properties at the saturation density and zero temperature; in these conditions the hyperons do not play any role and cannot influence the result.

We limit ourselves to the mean field approximation, in which the meson field operators are replaced by their expectation values; moreover, the ground state of the system we are interested in consists of static and uniform matter. This fact implies that the expectation values of the meson fields do not depend on time and space coordinates. At finite temperature the equations of motion for meson and nucleon fields are [33]

$$g_\sigma \sigma = \left(\frac{g_\sigma}{m_\sigma}\right)^2 \left[\frac{1}{\pi^2} \sum_B \int k^2 \frac{M_B - g_\sigma \sigma}{\sqrt{k^2 + (M_B - g_\sigma \sigma)^2}} \ f(\epsilon_B(\mathbf{k}), T) \ dk \ - b_M (g_\sigma \sigma)^2 - c(g_\sigma \sigma)^3 \right], \qquad (21)$$

$$g_\omega \omega_0 = \left(\frac{g_\omega}{m_\omega}\right)^2 \rho, \qquad\qquad m_\omega^2 \omega_k = 0, \qquad (22)$$

$$[\gamma_\mu (k^\mu - g_\omega \omega^\mu) - (M_B - g_\sigma \sigma)] \psi_B(k) = 0 \ , \qquad (23)$$

where ρ is the total baryon density given by

$$\rho \equiv \langle \psi^\dagger \psi \rangle = 2 \sum_B \int \frac{d\mathbf{k}}{(2\pi)^3} \ f(\epsilon_B(\mathbf{k}), T) \ , \qquad (24)$$

$f(\epsilon_B(\mathbf{k}), T) = \dfrac{1}{1 + \exp\left(\frac{\epsilon_B(\mathbf{k}) - \mu}{T}\right)}$ is the Fermi distribution function, and $\epsilon_B(\mathbf{k})$ is the fermion dispersion relation given by

$$\epsilon_B(\mathbf{k}) = g_\omega \omega_0 + \sqrt{k^2 + (M_B - g_\sigma \sigma)^2} \ . \qquad (25)$$

The pressure of nuclear matter is given by

$$\begin{aligned} p \ = \ &-\frac{1}{3} b_M (g_\sigma \sigma)^3 - \frac{1}{4} c (g_\sigma \sigma)^4 - \frac{1}{2} m_\sigma^2 \sigma^2 + \frac{1}{2} m_\omega^2 \omega_0^2 \\ &+ \frac{1}{3\pi^2} \sum_B \int \frac{k^2}{\sqrt{k^2 + (M_B - g_\sigma \sigma)^2}} \ f(\epsilon_B(\mathbf{k}), T) \ k^2 dk \ . \end{aligned} \qquad (26)$$

For the evaluation of the nuclear matter pressure at a given chemical potential and a given temperature we solve self-consistently Eqs. (21) and (24), obtaining the values of $g_\sigma \sigma$ and ρ that are used in Eq. (26).

When we compare the pressures of nuclear matter and quark matter, we face a normalization problem. As a matter of fact, at $T = \mu = 0$ the self-consistent solutions of Eqs. (21) and (24) are $\rho = 0$ and $g_\sigma \sigma = 0$, which imply $\omega_0 = 0$ by virtue of the equation of motion Eq. (22), and the vanishing of the phase space integral in Eq. (26). Clearly quark pressure must be lower than the nuclear one at relatively low values of density and/or temperature since in this region of parameters one is in the confined regime. The quark pressure, which is obtained by the thermodynamic potential Ω in Eq. (18) changing its sign, does not satisfy such a requirement. This problem is well known in NJL models [4], and the usual procedure is to subtract a positive constant B, the bag constant, from the quark pressure. The choice of B is not unique, and several different suggestions have been analyzed in the literature [4]. We choose to fix the bag constant by imposing that the transition temperature from nuclear to quark matter at zero chemical potential coincides with the crossover temperature T_Φ of the PNJL model discussed in the previous Section, i.e. the temperature where $d\Phi/dt$ has a maximum. In Table II we show the values of the bag constants and of T_Φ obtained for the various models. For each of the quark matter models considered here, the values of B obtained in comparison

	$B^{1/4}$ (MeV)	T_Φ (MeV)	μ_c stiff (MeV)	μ_c soft (MeV)
Polynomial, $T_0 = 270$ MeV	428.8	223	543	617
Polynomial, $T_0 = T_0(\mu)$	426.1	160	500	588
Logarithmic	425.6	153	490	566

TABLE II: Bag constants, deconfinement temperatures at $\mu = 0$ and deconfinement chemical potentials at $T = 0$ for the different quark matter models. Values of B obtained in comparison with soft and stiff nuclear matter differ of some part per thousand, therefore we show only one value of B for each quark matter model.
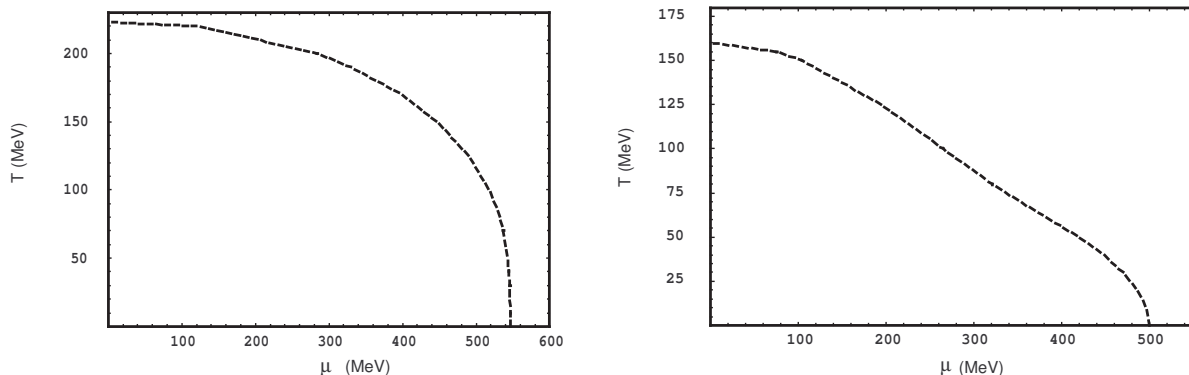

FIG. 4: Nuclear matter/quark matter phase diagrams in the PNJL model with $T_0 = 270$ MeV (left) and $T_0(\mu)$ (right). Nuclear matter contains hyperons and is described by the stiff equation of motion. Nuclear matter is favored in comparison with quark matter in the region below the line.

with soft and stiff nuclear matter differ of some part per thousand, therefore we show only one value of B for each quark matter model.

The results for the two cases are reported in Fig. 4. It shows the phase diagram obtained by comparing nuclear (with hyperons) and quark matter. The latter corresponds to the PNJL model with $T_0 = 270$ MeV (on the left panel) and $T_0 = T_0(\mu)$ (right panel). We stress that a more realistic treatment would require the introduction of different coupling constants in the baryon octet, but this is beyond the scope of the present study. The nuclear matter is chosen to be the one with the stiff equation of state (Set 2 of Table I). The transitions are of the first order. At $T = 0$ we find the critical quark chemical potential $\mu_c \approx 543$ and ≈ 500 MeV for the two cases. For the case of the logarithmic potential we find $\mu_c \approx 490$ MeV. If we replace the stiff nuclear matter with the soft one, the phase diagram is qualitatively the same as before; in this case we find $\mu_c \approx 617$ MeV, $\mu_c \approx 588$ MeV, $\mu_c \approx 566$ MeV, respectively for the polynomial potential with $T_0 = 270$ MeV, the polynomial potential with $T_0 = T_0(\mu)$ and the logarithmic potential.

A comparison with Fig. 1 shows that at small chemical potential the deconfinement temperature almost coincide with the chiral restoration temperature for the model with fixed T_0 (left panel in Fig.4), while for the μ-dependent T_0 (right panel in Fig.4) the two temperatures differ. Moreover, at small temperatures the critical baryonic chemical potential is higher for the deconfinement transition. However the values of the chemical potential found here are such that one of the color superconductive phases might be energetically favored [19, 20, 21, 22], a possibility we have not considered in the present paper for simplicity.

V. CONCLUSIONS

We have studied the phase diagram of the PNJL model with three flavors, considering different versions of the model, i.e. with polynomial and logarithmic forms of the Polyakov loop potential, in the former case with two forms of the reference temperature: T_0 fixed ($=270$ MeV) and μ-dependent $T_0(\mu)$. One result is related to the chiral symmetry phase transitions and is plotted in Fig. 1. In general we find at $\mu = 0$ crossover temperatures higher than the analogous result of the NJL model, namely $T = 175$ MeV. Moreover we find that the critical endpoint slightly depends on the choice of the model, but for all the cases considered in this paper the value of μ_E is higher than the result obtained by lattice QCD or QCD-like theories ($\mu_E \sim 50$ MeV). The PNJL result might be improved by adding

a new interaction term $\mathcal{O}(\bar{\psi}\psi)^4$ in the quark lagrangian as in Ref. [12]. We leave this investigation to a future project.

We have also studied the role of the Polyakov loop in the nuclei→quarks transition. In order to describe nuclear matter we have adopted the improved Walecka model with a self-interacting scalar field σ and a vector field ω_μ. We have chosen two sets of parameters of the nuclear matter lagrangian, corresponding respectively to a soft and to a stiff equation of state [33]. We find similar results in the two cases. The result of this analysis is summarized in Fig. 4 (stiff equation of state). The quark pressure is normalized by imposing that the deconfinement crossover of the PNJL model and the nuclei→quarks transitions occur at the same temperature at $\mu = 0$. We get that chiral symmetry restoration temperature and deconfinement temperature almost coincide at $T = 0$ in the case of fixed T_0 and polynomial form of the Polyakov loop potential, while for the μ-dependent T_0 the two temperatures differ. We also find that at small temperatures the critical chemical potential for deconfinement is higher than the one for the chiral transition, see Figs. 1 and 4.

This work might be improved in several different ways. For example one should impose electric and color neutrality in the quark matter sector. Also the possibility of a color superconductive phase at high density should be taken into account. Moreover the nuclear matter equation of state should be replaced by a more sophisticated one taking into account population imbalances due to β−equilibrium and electric neutrality. We leave all these issues to future projects. We finally note that while preparing this text we became aware of an almost simultaneous and independent study of the three flavor PNJL model [34] that has some overlap with our work.

[1] Y. Nambu and G. Jona-Lasinio, Phys. Rev. **122**, 345 (1961); Phys. Rev. **124**, 246 (1961).

[2] S. P. Klevansky, Rev. Mod. Phys. **64**, 649 (1992); T. Hatsuda and T. Kunihiro, Phys. Rept. **247**, 221 (1994) [arXiv:hep-ph/9401310]; M. Buballa, Phys. Rept. **407**, 205 (2005) [arXiv:hep-ph/0402234].

[3] S. Lawley, W. Bentz and A. W. Thomas, J. Phys. G **32**, 667 (2006) [arXiv:nucl-th/0602014].

[4] P. Wang, A. W. Thomas and A. G. Williams, Phys. Rev. C **75**, 045202 (2007) [arXiv:nucl-th/0610084]; N. Ippolito, M. Ruggieri, D. Rischke, A. Sedrakian and F. Weber, arXiv:0710.3874 [astro-ph]; F. Sandin and D. Blaschke, Phys. Rev. D **75**, 125013 (2007) [arXiv:astro-ph/0701772]; M. Alford and S. Reddy, Phys. Rev. D **67**, 074024 (2003) [arXiv:nucl-th/0211046]; M. Alford, M. Braby, M. W. Paris and S. Reddy, Astrophys. J. **629**, 969 (2005) [arXiv:nucl-th/0411016].

[5] K. Fukushima, Phys. Lett. B **591**, 277 (2004) [arXiv:hep-ph/0310121].

[6] A. M. Polyakov, Phys. Lett. B **72**, 477 (1978); L. Susskind, Phys. Rev. D **20**, 2610 (1979); B. Svetitsky and L. G. Yaffe, Nucl. Phys. B **210**, 423 (1982); B. Svetitsky, Phys. Rept. **132**, 1 (1986).

[7] A. Gocksch and M. Ogilvie, Phys. Rev. D **31**, 877 (1985);E. M. Ilgenfritz and J. Kripfganz, Z. Phys. C **29**, 79 (1985); S. Digal, E. Laermann and H. Satz, Eur. Phys. J. C **18**, 583 (2001) [arXiv:hep-ph/0007175]; K. Fukushima, Phys. Lett. B **553**, 38 (2003) [arXiv:hep-ph/0209311]; K. Fukushima, Phys. Rev. D **68**, 045004 (2003) [arXiv:hep-ph/0303225]; F. Sannino, Phys. Rev. D **66**, 034013 (2002) [arXiv:hep-ph/0204174]; Y. Hatta and K. Fukushima, Phys. Rev. D **69**, 097502 (2004) [arXiv:hep-ph/0307068]; A. Mocsy, F. Sannino and K. Tuominen, Phys. Rev. Lett. **92**, 182302 (2004) [arXiv:hep-ph/0308135].

[8] M. Fukugita and A. Ukawa, Phys. Rev. Lett. **57**, 503 (1986); A. Barducci, R. Casalbuoni, S. De Curtis, R. Gatto, G. Pettini, Phys. Lett. **B244**, 311 (1990); F. Karsch and E. Laermann, Phys. Rev. D **50**, 6954 (1994) [arXiv:hep-lat/9406008]; S. Aoki *et al.* [JLQCD Collaboration], Phys. Rev. D **57**, 3910 (1998) [arXiv:hep-lat/9710048]; F. Karsch, E. Laermann and A. Peikert, Nucl. Phys. B **605**, 579 (2001) [arXiv:hep-lat/0012023]; C. R. Allton *et al.*, Phys. Rev. D **66**, 074507 (2002) [arXiv:hep-lat/0204010]; P. N. Meisinger and M. C. Ogilvie, Nucl. Phys. Proc. Suppl. **47**, 519 (1996) [arXiv:hep-lat/9509050]; P. N. Meisinger and M. C. Ogilvie, Phys. Lett. B **379**, 163 (1996) [arXiv:hep-lat/9512011].

[9] C. Ratti, M. A. Thaler and W. Weise, Phys. Rev. D **73**, 014019 (2006) [arXiv:hep-ph/0506234].

[10] S. Roessner, C. Ratti and W. Weise, Phys. Rev. D **75**, 034007 (2007) [arXiv:hep-ph/0609281].

[11] S. K. Ghosh, T. K. Mukherjee, M. G. Mustafa and R. Ray, arXiv:0710.2790 [hep-ph]; S. K. Ghosh, T. K. Mukherjee, M. G. Mustafa and R. Ray, Phys. Rev. D **73**, 114007 (2006) [arXiv:hep-ph/0603050].

[12] K. Kashiwa, H. Kouno, M. Matsuzaki and M. Yahiro, arXiv:0710.2180 [hep-ph].

[13] B. J. Schaefer, J. M. Pawlowski and J. Wambach, Phys. Rev. D **76**, 074023 (2007) [arXiv:0704.3234 [hep-ph]].

[14] C. Ratti, S. Roessner and W. Weise, Phys. Lett. B **649**, 57 (2007) [arXiv:hep-ph/0701091].

[15] C. Sasaki, B. Friman and K. Redlich, Phys. Rev. D **75**, 074013 (2007) [arXiv:hep-ph/0611147]; C. Sasaki, B. Friman and K. Redlich, Phys. Rev. D **75**, 054026 (2007) [arXiv:hep-ph/0611143].

[16] E. Megias, E. Ruiz Arriola and L. L. Salcedo, Phys. Rev. D **74**, 114014 (2006) [arXiv:hep-ph/0607338]; E. Megias, E. Ruiz Arriola and L. L. Salcedo, Phys. Rev. D **74**, 065005 (2006) [arXiv:hep-ph/0412308].

[17] M. Ciminale, G. Nardulli, M. Ruggieri and R. Gatto, arXiv:0706.4215 [hep-ph].

[18] M. G. Alford, K. Rajagopal and F. Wilczek, Nucl. Phys. B **537**, 443 (1999) [arXiv:hep-ph/9804403].

[19] D. H. Rischke, D. T. Son and M. A. Stephanov, Phys. Rev. Lett. **87**, 062001 (2001) [arXiv:hep-ph/0011379]; M. G. Alford, K. Rajagopal and F. Wilczek, Phys. Lett. B **422**, 247 (1998) [arXiv:hep-ph/9711395]; R. Rapp, T. Schafer, E. V. Shuryak and M. Velkovsky, Phys. Rev. Lett. **81**, 53 (1998) [arXiv:hep-ph/9711396].

[20] S. B. Ruster, V. Werth, M. Buballa, I. A. Shovkovy and D. H. Rischke, Phys. Rev. D **72**, 034004 (2005) [arXiv:hep-ph/0503184].

[21] D. Blaschke, S. Fredriksson, H. Grigorian, A. M. Oztas and F. Sandin, Phys. Rev. D **72**, 065020 (2005) [arXiv:hep-ph/0503194].

[22] N. D. Ippolito, G. Nardulli and M. Ruggieri, JHEP **0704**, 036 (2007) [arXiv:hep-ph/0701113].

[23] M. LeBellac, *Thermal Field Theory* (Cambridge University Press, 1996).

[24] O. Kiriyama, M. Maruyama and F. Takagi, Phys. Rev. D **62**, 105008 (2000) [arXiv:hep-ph/0001108].

[25] O. Kiriyama, M. Maruyama and F. Takagi, Phys. Rev. D **63**, 116009 (2001) [arXiv:hep-ph/0101110].

[26] Y. Hashimoto, Y. Tsue and H. Fujii, Prog. Theor. Phys. **114**, 595 (2005) [arXiv:hep-ph/0506017].

[27] Y. Aoki, Z. Fodor, S. D. Katz and K. K. Szabo, JHEP **0601**, 089 (2006) [arXiv:hep-lat/0510084]; Y. Aoki, Z. Fodor, S. D. Katz and K. K. Szabo, Phys. Lett. B **643**, 46 (2006) [arXiv:hep-lat/0609068]; Z. Fodor and S. D. Katz, JHEP **0404**, 050 (2004) [arXiv:hep-lat/0402006]; C. R. Allton, S. Ejiri, S. J. Hands, O. Kaczmarek, F. Karsch, E. Laermann and C. Schmidt, Phys. Rev. D **68**, 014507 (2003) [arXiv:hep-lat/0305007]; C. Bernard *et al.*, Phys. Rev. D **75**, 094505 (2007) [arXiv:hep-lat/0611031].

[28] R. A. Lacey, N. N. Ajitanand, J. M. Alexander, P. Chung, J. Jia, A. Taranenko and P. Danielewicz, arXiv:0708.3512 [nucl-ex].

[29] A. Dumitru, Y. Hatta, J. Lenaghan, K. Orginos and R. D. Pisarski, Phys. Rev. D **70**, 034511 (2004) [arXiv:hep-th/0311223].

[30] A. Dumitru, R. D. Pisarski and D. Zschiesche, Phys. Rev. D **72**, 065008 (2005) [arXiv:hep-ph/0505256].

[31] J. D. Walecka, Annals Phys. **83**, 491 (1974).

[32] J. Boguta and A. R. Bodmer, Nucl. Phys. A **292**, 413 (1977).

[33] N. K. Glendenning, *Compact stars: Nuclear physics, particle physics, and general relativity* (Springer, New York, 1997)

[34] W. Fu, Z. Zhang and Y. Liu, arXiv:0711.0154 [hep-ph].